

Electronic and dynamical properties of Si/Ge core-shell nanowires

H. Peelaers,^{*} B. Partoens, and F. M. Peeters[†]

Departement Fysica, Universiteit Antwerpen, Groenenborgerlaan 171, B-2020 Antwerpen, Belgium

(Received 11 June 2010; revised manuscript received 8 September 2010; published 29 September 2010)

Full *ab initio* techniques are applied to study the electronic and dynamical properties of free standing, hydrogen-passivated Si/Ge core-shell nanowires oriented along the [110] direction. All studied wires exhibit a direct band gap and are found to be structurally stable. The different contributions of the core and shell atoms to the phonon spectra are identified. The acoustic phonon velocities and the frequencies of some typical optical modes are compared with those of pure Si and Ge nanowires. These depend either on the concentration or on the type of core material. Optical modes are hardened and longitudinal acoustic velocities are softened with decreasing wire diameter.

DOI: [10.1103/PhysRevB.82.113411](https://doi.org/10.1103/PhysRevB.82.113411)

PACS number(s): 62.23.Hj, 63.22.Gh, 61.46.Km

Semiconducting nanowires are one-dimensional structures that have generated a lot of interest lately due to their promising applications as potential building blocks for nanodevices. Coaxial Si/Ge heterostructures of such wires can readily be made.¹⁻⁵ Due to the sharp interface between the Ge core and the Si shell and the valence-band offset, the interface will serve as a confinement potential, so that a one-dimensional hole gas can be created in undoped structures.³ Additionally the Si shell can be used to create transparent contacts. Due to these properties, these heterostructures can be used as high switching speed transistors² and field-effect transistors.⁴ *P-i-n* type heterostructures have already shown applications as solar cells.⁶

Changing the sizes of the core and shell regions allows one to engineer the band gaps, as was shown experimentally⁵ and theoretically.⁷⁻⁹ The effect of band offsets and the spatial confinement of carriers in Si/Ge and *p-i-n* types of core-shell nanowires was also treated theoretically.¹⁰⁻¹² The atomic structure of these wires can experimentally be studied by using transmission electron microscopy but knowledge of the phonon spectra can lead to a characterization based on Raman spectroscopy. A first theoretical step in the understanding of the lattice dynamics of Si/Ge core-shell structures has been made using the empirical valence force-field model containing two- and three-body interactions¹³ to study the phonon spectra and the specific heat in these wires. Here, we go a step further and use a full *ab initio* approach to study *both* the electronic and the dynamical properties of Si/Ge core-shell nanowires and compare these results with those of Si or Ge nanowires. We restrict ourselves to structures that are oriented in the [110] direction and are hydrogen passivated.

The calculations presented here are performed within density-functional theory for the electronic part and density functional perturbation theory¹⁴ for the dynamical part, using the ABINIT software package.¹⁵ The local density approximation (LDA) is used to describe the exchange-correlation potentials. We used Troullier-Martins pseudopotentials¹⁶ with an energy cutoff of 20 Ha. A supercell approach is used to describe the properties of the free standing nanowires by utilizing a sufficient vacuum layer between the nanowire and its neighboring images. A $1 \times 1 \times 16$ shifted Monkhorst-Pack¹⁷ grid was used for the *k*-point integrations and all wires were relaxed so that the maximum

force component is smaller than 5×10^{-5} Hartree/Bohr and that all components of the stress tensor are smaller than 5×10^{-7} Hartree/Bohr³.

In this work we study two different sized nanowires with a diameter of 1.2 and 1.6 nm, both of them hydrogen passivated. For each of these diameters either a wire with a core composed of Si or Ge will be constructed. For the 1.6 nm nanowire two different shell sizes are considered. A cross section of the resulting relaxed structures in case of a Ge core is shown in Fig. 1. In the following we label these wires as core shell a, b, and c. The reverse structures (i.e., where Ge is replaced with Si and vice versa) are also studied.

In order to understand the modification of the electronic band structure due to the presence of a core, we considered as an example the case of a Ge core and show in Fig. 2 the energy band structures. Wires with Si core have similar band structures. Notice that all core-shell structures have a direct band gap [values are plotted in Fig. 3(a)], which is similar for Si and Ge nanowires and confirms earlier results.⁸ Starting from a pure nanowire (either a Si or Ge one) and adding a core of the second material leads to a smaller band gap due to quantum confinement effects¹² in these small nanowires and due to the strain on the core atoms⁹ induced by the difference in lattice constant between Si and Ge. This strain

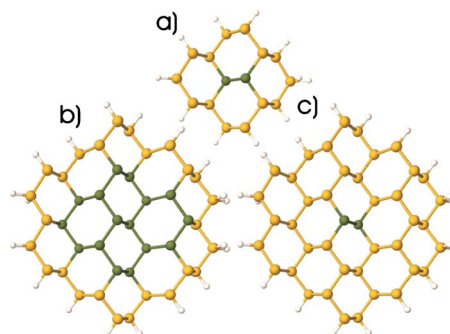


FIG. 1. (Color online) Relaxed unit cell of three different nanowires oriented along the [110] direction, all with a Ge core: (a) a 1.2 nm [110] wire with a core of 2 Ge atoms (green color), a shell of 14 Si atoms (yellow color), and a passivating layer of 12 H atoms (white color), (b) a 1.6 nm nanowire with 16 Ge core atoms, 26 Si shell atoms, and 20 passivating H atoms, and (c) 1.6 nm wire with 2 Ge core atoms, 40 Si shell atoms, and 20 H atoms.

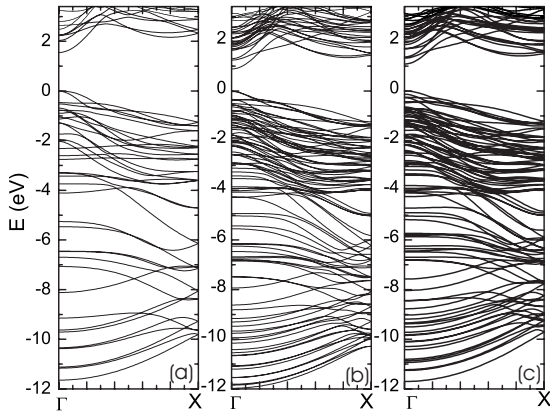


FIG. 2. Band structure of Ge core nanowires corresponding to the structures depicted in Fig. 1.

effect will also be present in thicker nanowires. If one also takes into account that pure Si nanowires have a larger band gap than comparable sized pure Ge nanowires, one can explain Fig. 3(a) completely. It is well known that the LDA underestimates the band gaps but all relative trends are predicted correctly. In Figs. 3(b) and 3(c), respectively, the effective electron and hole band mass are plotted as function of the concentration and structure type. The electron effective mass is almost independent of the wire type and wire diameter. The hole effective mass strongly depends on the type of structure and of the wire size.

Next we calculate the dynamical properties and present the phonon energies as function of the wavevector in Fig. 4 for the three nanowires shown in Fig. 1. Notice that the low frequency (acoustic) modes around Γ exhibit typical one-dimensional features: four acoustic modes of which two are linear in q_z and two are quadratic in q_z .¹⁸ All calculated phonon spectra have only real frequencies and thus all structures can be considered stable (as the occurrence of imaginary frequencies would indicate a structural instability). To directly compare these spectra, it is useful to calculate the phonon density of states (DOS). We used a box counting method where the frequencies were smeared by gaussians (with full width at half maximum of 10 cm^{-1}). Figure 5 shows the DOS of core shell b [see Fig. 1(b)]. It is instructive to

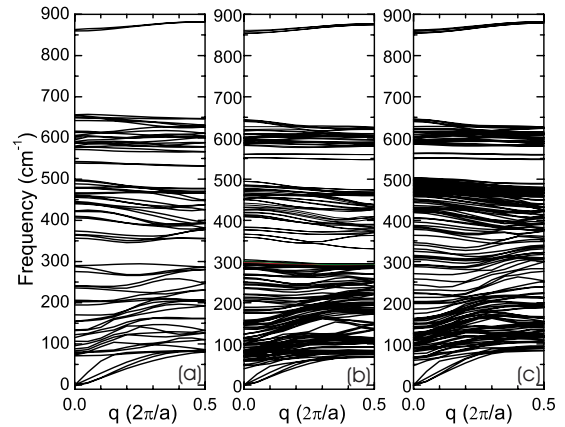


FIG. 4. (Color online) The phonon spectra of the Ge core nanowires corresponding to the structures depicted in Fig. 1. Frequencies higher than 900 cm^{-1} are not shown.

compare this DOS with the DOS of pure nanowires. In Fig. 5(a) the DOS of a pure 1.6 nm SiNW (Ref. 18) is also added (red dashed line) while in Fig. 5(b) the DOS of a pure 1.6 nm GeNW (Ref. 19) (black dashed line) and also of the core-shell structure c (red dotted line) is added. When comparing the DOS of the core-shell structure b with the one from either the Si or Ge nanowire, one can immediately identify which type of atoms (Si or Ge) are present in the shell, as the Si-H and Ge-H stretching modes (with frequencies around 2000 cm^{-1}) have different frequencies. The same observation can be made for the bending modes (frequencies around 870 and 600 cm^{-1}), which in this case is determined by the Si shell. Both the DOS for the pure Si and Ge nanowire have a characteristic peak, 290 cm^{-1} for pure Ge (labeled I in Fig. 5) and one around 480 cm^{-1} for pure Si (labeled II in Fig. 5). The effect of the core atoms is observable as a lowering of this Ge peak (peak I) and an increase in the Si contribution around 480 cm^{-1} (peak II). In core-shell structure c the number of Ge atoms in the core is small compared to those in the core-shell structure b (just two Ge atoms), which shows up as a decrease of the Ge peak (peak I) in the DOS [Fig. 5(b)] and an increase in the Si peak (peak II).

Next we look into more detail to some specific modes with their associated energies. In order to do this the acoustic

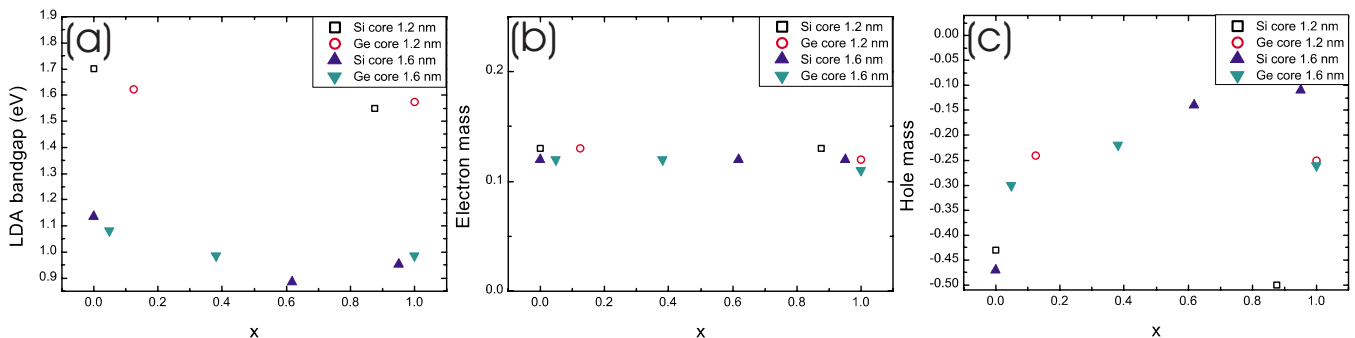


FIG. 3. (Color online) (a) LDA band gap, (b) electron effective band mass, and (c) hole effective band mass. Each type of core-shell structure has a different symbol (depending on wire size and type of core atoms). The x axis depicts the concentration of Ge atoms, where 0 indicates the absence of Ge atoms (a pure Si nanowire) and 1 a wire only consisting of Ge.

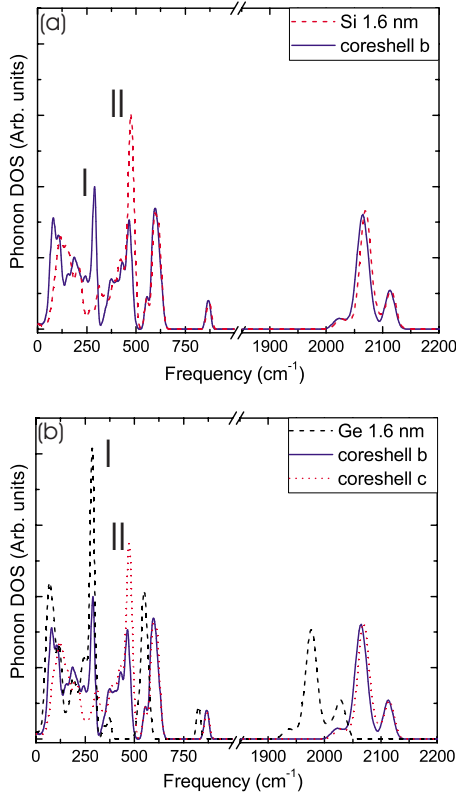


FIG. 5. (Color online) The phonon DOS of Ge core nanowires: (a) comparison between the core-shell structure b and a pure Si nanowire and (b) comparison between the core-shell structure b, a pure Ge nanowire, and the core-shell structure c. The peak labeled I is a typical Ge peak while the peak labeled II is a typical Si peak.

phonon velocities [calculated for the transversal (rotational) (v_T) and longitudinal mode (v_L)], the first optical frequency (ω_σ), the bending mode around 600 cm^{-1} (ω_1) and the breathing mode (ω_b) are plotted in Fig. 6 as function of wire type (different symbols) and concentration of Ge (x axis, ranging from 0, equal to no Ge at all, to 1, meaning only Ge atoms). Different dependencies can be observed: some properties (e.g., the transversal velocity v_T) only depend on the Ge concentration and not on the specific structure (i.e., the velocity does not depend on the type of atom in the core), while other frequencies (e.g., the bending mode ω_1) only depend on the type of atoms near the edges, which can be explained by the fact that these frequencies correspond to a Si-H or Ge-H bending mode. For the other properties the distinction between the two is not that clear. For the breathing mode ω_b it is rather the concentration that is important while for the first optical frequency ω_σ and the longitudinal velocity v_L the type of wire is important which can be seen by the different behavior of the Si core versus the Ge core.

The hardening of optical frequencies and the softening of the acoustic frequencies (especially in case of the longitudinal velocity) with decreasing wire diameter, which was observed for both Si and Ge nanowires^{18,19} is also present in the core-shell structures, as can be seen by comparing the obtained values for the 1.2 nm with the 1.6 nm nanowire.

In conclusion, we have performed an *ab initio* study of the electron spectrum and the phonons in Si/Ge core-shell nanowires. The obtained electronic properties are in accordance with previous theoretical studies. Using the calculated phonon spectra we showed that all studied structures are stable and that the calculated DOS can be used to distinguish

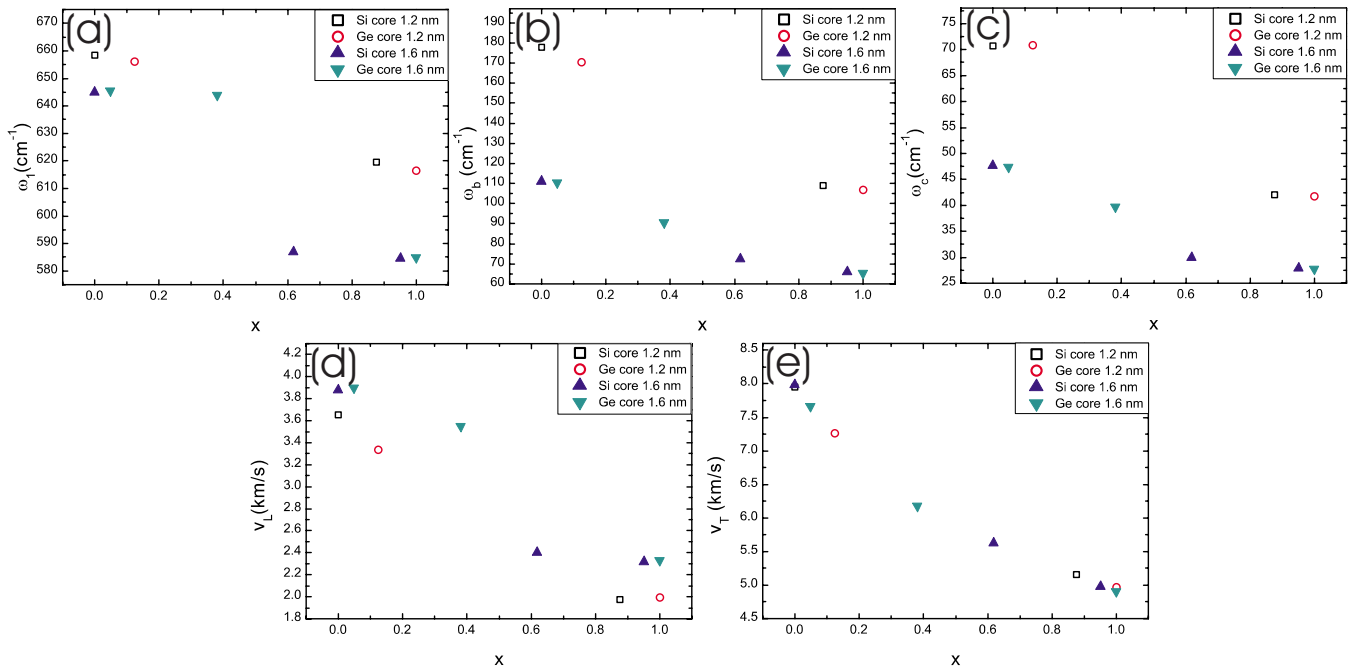


FIG. 6. (Color online) (a) The frequency of the breathing mode ω_b , (b) the frequency of the first optical mode ω_σ , (c) the frequency of the optical mode around 600 cm^{-1} ω_1 , (d) the transversal sound velocity v_T , and (e) the longitudinal sound velocity v_L . Each type of core-shell structure has a different symbol (depending on wire size and type of core atoms). The x axis depicts the concentration of Ge atoms, where 0 indicates the absence of Ge atoms (a pure Si nanowire) and 1 a wire only consisting of Ge.

between the different core-shell types, e.g., it can be used to determine the core and shell materials and their relative concentrations. The optical frequencies and acoustic velocities for different core-shell structures are shown as a function of the Ge concentration. The transversal acoustic velocity only depends on the Ge concentration while the core-shell structure determines the frequencies of the bending modes.

Hardening of optical modes and softening of longitudinal acoustic velocities is observed with decreasing wire diameter.

This work was supported by the Flemish Science Foundation (FWO-VI), the Belgian Science Policy (IAP), and NOI-BOF (University of Antwerp).

*hartwin.peelaers@ua.ac.be

†francois.peeters@ua.ac.be

¹L. J. Lauhon, M. S. Gudixsen, D. Wang, and C. M. Lieber, *Nature (London)* **420**, 57 (2002).

²Y. Hu, J. Xiang, G. Liang, H. Yan, and C. M. Lieber, *Nano Lett.* **8**, 925 (2008).

³W. Lu, J. Xiang, B. P. Timko, Y. Wu, and C. M. Lieber, *Proc. Natl. Acad. Sci. U.S.A.* **102**, 10046 (2005).

⁴J. Xiang, W. Lu, Y. Hu, Y. Wu, H. Yan, and C. M. Lieber, *Nature (London)* **441**, 489 (2006).

⁵J.-E. Yang, C.-B. Jin, C.-J. Kim, and M.-H. Jo, *Nano Lett.* **6**, 2679 (2006).

⁶B. Tian, X. Zheng, T. J. Kempa, Y. Fang, N. Yu, G. Yu, J. Huang, and C. M. Lieber, *Nature (London)* **449**, 885 (2007).

⁷R. N. Musin and X.-Q. Wang, *Phys. Rev. B* **71**, 155318 (2005).

⁸R. N. Musin and X.-Q. Wang, *Phys. Rev. B* **74**, 165308 (2006).

⁹X. Peng and P. Logan, *Appl. Phys. Lett.* **96**, 143119 (2010).

¹⁰A. Nduwimana, R. N. Musin, A. M. Smith, and X.-Q. Wang,

Nano Lett. **8**, 3341 (2008).

¹¹A. Nduwimana and X.-Q. Wang, *Nano Lett.* **9**, 283 (2009).

¹²M. Amato, M. Palummo, and S. Ossicini, *Phys. Rev. B* **79**, 201302 (2009).

¹³Y. Zhang and Y. Xiao, *Eur. Phys. J. B* **63**, 425 (2008).

¹⁴S. Baroni, S. de Gironcoli, A. Dal Corso, and P. Giannozzi, *Rev. Mod. Phys.* **73**, 515 (2001).

¹⁵X. Gonze, J.-M. Beuken, R. Caracas, F. Detraux, M. Fuchs, G.-M. Rignanese, L. Sindic, M. Verstraete, G. Zerah, F. Jollet, M. Torrent, A. Roy, M. Mikami, Ph. Ghosez, J.-Y. Raty, and D. C. Allen, *Comput. Mater. Sci.* **25**, 478 (2002).

¹⁶N. Troullier and J. L. Martins, *Phys. Rev. B* **43**, 1993 (1991).

¹⁷H. J. Monkhorst and J. D. Pack, *Phys. Rev. B* **13**, 5188 (1976).

¹⁸H. Peelaers, B. Partoens, and F. M. Peeters, *Nano Lett.* **9**, 107 (2009).

¹⁹H. Peelaers, B. Partoens, and F. M. Peeters, *Appl. Phys. Lett.* **95**, 122110 (2009).